# Status Of The Integrated Topping Cycle MHD Generator Testing

Author(s): C. C. P. Pian, A. W. Dunton, E. W. Schmitt, D. J. Morrison, and L. C. Farrar

Session Name: Proof-of-Concept Testing

SEAM: 31 (1993)

SEAM EDX URL: https://edx.netl.doe.gov/dataset/seam-31

EDX Paper ID: 1608

# STATUS OF THE INTEGRATED TOPPING CYCLE MHD GENERATOR TESTING*

C.C.P. Pian, A.W. Dunton, E.W. Schmitt, and D.J. Morrison
Textron Defense Systems/Subsidiary of Textron, Inc.
Everett, Massachusetts 02149

and

L.C. Farrar
Montec Associates, Inc.
Butte, Montana 59702

## ABSTRACT

The status of the Integrated Topping Cycle (ITC) MHD generator testing is presented. This generator is part of a 50 $MW_t$ prototypic powertrain that is currently undergoing proof-of-concept (POC) testing at the U.S. Department of Energy's Component Development and Integration Facility in Butte, Montana. Test objectives are to establish component lifetimes at prototypic operating conditions and to verify the design performance parameters.

The ITC generator has completed Design Verification Testing and is now well into the POC duration test. To date (May 1, 1993), over 360 hours of the planned 1000 hours of testing has been completed. Generator testing is being performed at conditions representative of commercial power plant operating conditions. Prototypic generator channel hardware is performing very well. Based on test results obtained thus far, the prognosis is excellent for meeting all of the POC test objectives.

## I. INTRODUCTION

The status of the Integrated Topping Cycle MHD generator testing is presented in this paper. This generator is a part of a 50 $MW_t$ prototypic powertrain that is currently undergoing proof-of-concept testing at the U.S. Department of Energy's Component Development and Integration Facility (CDIF) in Butte, Montana. The POC test is planned for 1000 hours duration, with the test objectives being to establish component lifetimes at prototypic operating conditions and to verify the design performance parameters. The ITC generator has completed Design Verification Testing (DVT) and is now well into the POC duration test. A summary of the MHD generator performance characteristics and hardware evaluations are provided herein.

The purpose of the DVT was to establish nominal operating conditions for the POC duration test, to confirm that the powertrain components meet the performance objectives of the Statement-of-Work (SOW), and to identify any generator hardware "infant mortality" problems.

Design Verification Testing was originally scheduled to be accomplished in 50 hours.[1] However, because of inconclusive results, the test series was extended. The first part of the DVT series (the initial 50 hours) took place in September 1992, and the second between January and March 1993. Long duration POC testing commenced in April 1993.

*This work was sponsored by the U.S. Department of Energy under Contract No. DE-AC22-87PC90274 and funded through TRW, Inc. under Subcontract No. CX136D58S.

Most of the early DVT was dedicated to troubleshooting an extensively modified test facility (a "shakedown" period), establishing combustor operating parameters, and studying the effects of combustor hardware configuration changes. It also provided, for the first time, a means to test all the newly installed integrated power train components.

The later DVT series was aimed primarily at determining the effects of various changes, in both hardware and operating parameters identified during early DVT, on overall channel performance and hardware reliability. On the basis of these tests, a set of nominal combustor operating conditions was chosen. Also, a modified segmented diffuser loading scheme was implemented.

As of May 1, 1993, a total of 360 hours of coal-fired operation have been accumulated with the $1A_4$ generator channel, including approximately 200 hours at the design power operating conditions. Channel reliability has been excellent, despite often abnormally harsh operating conditions from the aforementioned "shakedown" periods during the early DVT series. The SOW generator performance level and the prototypic channel wall stress conditions have been achieved at the nominal power train operating conditions.

This paper primarily addresses performance and hardware evaluations of the channel, nozzle and diffuser. Results of the coal-fired combustor and current control devices are discussed in References 2 and 3, respectively. The performance characteristics of the $1A_4$ generator during the DVT series are discussed in Section II, followed by a report on the conditions of the channel hardware in Section III. The operating characteristics of the generator during duration testing are discussed in Section IV.

## II. PERFORMANCE CHARACTERISTICS

A summary of the generator performance throughout the DVT series is presented in this section. Included are: 1) a comparison of electrical conductivity measured early and late in the DVT series, 2) a comparison between pretest predicted performance and measured data, and 3) a comparison of fluctuations in the measured generator electrical variables for different powertrain operating conditions.

### Electrical Conductivity Measurements

Many conductivity measurements made early in the DVT series were lower than expected. The investigation described below indicated that combustor and facility modifications during the DVT have resulted in considerable improvement in measured conductivity. The degree of improvement is quantified through comparison with calculated model results.

Plasma conductivity is measured using a dc power supply connected between the nozzle and the diffuser. The plasma conductivity at a given axial location is proportional to the measured power supply current and inversely proportional to the measured interelectrode voltage. Figure 1 shows a typical axial profile of plasma conductivity, determined in this manner.

Also shown in Figure 1 are calculated electrical conductivity profiles using different values of the conductivity multiplication factor (sigfac). The value of sigfac required to scale the calculated profile to match the test data can be used as a measure of the combustion efficiency, seed utilization, and other factors affecting plasma conductivity. Second stage oxidizer mixing also affects the slope of measured conductivity profiles. When mixing was poor, as was often the case during early DVT, measured conductivity profiles tended to be flatter than calculations would predict.

Figure 2 shows the measured power supply currents during early DVT tests investigating different first-stage combustor stoichiometries and overall oxidant N-to-O ratios. The bulk conductivities of the plasma are directly proportional to the measured power supply currents since the same power supply voltage was used in all measurements. Computer calculations of conductivity were also carried out for these operating conditions. The best agreements with data were obtained for calculations with a sigfac of approximately 0.7. In contrast, a sigfac of approximately 0.9 has typically been required to match the conductivity data from the $1A_1$ workhorse generator tests.

Figure 3 compares measured power supply currents from both early and late DVT test series. The improved conductivity in the later DVT data is primarily the result of changes in the global combustion equivalence ratio and in the hardware configuration of the coal-fired precombustor. The best agreement with later DVT data was for calculated conductivities using a sigfac of 0.88.

## Comparison of Pretest Prediction with Measured Generator Performance

A preliminary comparison is made between a pretest generator performance prediction and actual DVT measurements. A generator operating condition during test 92-DVT-10 was selected for the performance comparison. This test condition was selected because it had nearly identical generator performance as the Proof-of-Concept "Stress" Reference Operating Conditions (ROC) specified in the test plan.[1] Table 1 compares the predicted and measured generator performance. The calculated results matched well with the measured data. The axial distributions of various measured electrical variables also agreed well with the calculated profiles, as shown in Figure 4.

Although the calculated and measured generator performances are similar, the process flow parameters and the amount of combustor heat loss assumed in the pretest calculations were different from those obtained during the DVT, as seen in Table 1. One possible explanation for the close agreement between the calculated and measured results is that, even though the upstream combustor heat losses and seed fraction were different, the plasma electrical conductivity during the test was similar to that of the calculation. To see if this was indeed the case, pretest conductivity calculations were compared to estimates of conductivity from test 92-DVT-10. The plasma electrical conductivity at the nozzle throat in the pre-test calculation was 7.5 mhos/m. Conductivity was not measured during the 92-DVT-10 test, but the electrical conductivity at the nozzle throat can be estimated from computer analyses to be approximately 6.5 mho/m. This conductivity value is determined by extending the calculated conductivity profile (which best matched data at mid-channel) forward to the nozzle throat, as shown earlier in Figure 1.

The $1A_4$ generator produced 1.0 MW of electrical power with a plasma conductivity of less than 6.5 mhos/m (at the nozzle throat) during the power test 92-DVT-10. On the other hand, the pretest analysis predicted a conductivity value of 7.5 mho/m would be necessary to produce the same power. This suggests that the amount of current leakage assumed in the pretest analysis was too high. The approach adopted for modeling the wall leakage was similar to that used earlier in Reference 4, which in effect also accounts for other power loss mechanisms not specifically included in the model (such as flow nonuniformities and poor mixing). The assumed axial leakage current was more than 120A at a mid-channel location. The high wall current leakage estimate compensated for the higher inlet conductivity and resulted in a lower calculated power output. Therefore with less axial current leakage and a nozzle throat conductivity of 7.5 mhos/m, the $1A_4$ generator should be able to produce substantially more power than the pretest prediction of 1.0 MW.

## Voltage and Current Fluctuations

Substantial fluctuations were observed in the measured generator power output, the diagonal load current (with time) and the interanode voltage distribution (with time and space) during the DVT series. The magnitudes of these fluctuations were considerably higher than those observed during earlier $1A_1$ workhorse generator tests. Such unsteady generator operation is a source of concern, since the $1A_4$ generator channel is being subjected to potentially damaging electrical stresses under these circumstances. These electrical stresses are more severe than what is considered to be prototypic.

The causes of the unsteadiness are under investigation, but prime candidates include unsteady process flows and reduced combustion efficiency.[2,5] The generator's electrical output data, measured at various intervals during the DVT series, were examined in order to compare the fluctuations for different combustor operating configurations and after facility modifications. Some general trends concerning factors affecting the fluctuations were observed. The amount of electrical fluctuation appeared to be particularly sensitive to the steadiness of the coal feed and air oxidant systems. Generator fluctuations also tended to change with different combustor configurations and operating conditions. In general, the generator tended to operate more smoothly with increasing combustor equivalence ratio, with higher power output, with higher stoichiometry in the precombustor can, and with improved second-stage mixing.[2]

Some examples of interanode voltage and load current fluctuations for different combustor operating conditions are compared in Figures 5 through 7. The measured interanode voltage (IAV) profiles for different 2nd stage configurations are compared in Figure 5. Figures 5(a) and 5(b) show typical IAV's from tests 93-DVT-8 and 93-DVT-36, respectively. All

the combustor operating conditions for the two tests were comparable, except the latter test had a higher equivalence ratio in the coal-fired precombustor can which improved overall combustion efficiency and which resulted in better flow mixing in the second stage duct. This was evident from the higher measured second stage heat loss (an indication of better burning) during 93-DVT-36. The figures show the mean values of the interanode gap voltages (averaged over one minute) in the mid-channel region, as well as the standard deviation of each voltage over the same time period. Not only are the mean values in 93-DVT-8 scattered about more, but the deviation of each interanode voltage is much greater than in 93-DVT-36. In addition, several of the IAV's ranged from negative to positive over the course of a minute.

In order to quantify the magnitude of IAV fluctuations for a specific generator channel region, the spatial standard deviation for a group of interanode voltages at a given time was normalized by the mean voltage of that same group, and the result examined over time. This variable (for k interanode gaps ranging from anodes n to n+k) is given by the following expression:

$$\chi_{\text{n to (n+k)}} = \frac{\text{Standard Deviation } [IAV_{\text{n to (n+k)}}]}{\text{Mean } [IAV_{\text{n to (n+k)}}]}$$

Figure 6 shows typical time histories of $\chi$ for anodes 151-160 during the tests referenced in Figure 5. Both the mean and amplitude of $\chi$ during test 93-DVT-8 were much greater than in 93-DVT-36. This behavior indicates large spatial variations between adjacent IAV's, as well as large temporal variations among the individual IAV's. These variations suggest the initiation and quenching of strong arcs (both Faraday and Hall arcs) at the anode wall. The low level of IAV fluctuations during test 93-DVT-36 is comparable to that obtained during the earlier $1A_1$ workhorse testing.

The sensitivity of load current fluctuations to equivalence ratio is shown in Figure 7. Figure 7(a) shows the time history of the measured load current from test 93-DVT-7, during which the combustion equivalence ratio was increased. Figure 7(b) shows the time variations of a parameter $\tau$, which is used to quantify the load current fluctuation. $\tau$ is defined as follows:

$$\tau_{\text{(t=1 min.)}} = \frac{\text{Standard Deviation [load current]}_{\text{(t=1 min.)}}}{\text{Mean [load current]}_{\text{(t=1 min.)}}}$$

It is apparent from this early DVT series result that $\tau$ (and therefore the amount of load current fluctuations) decreased substantially when the equivalence ratio was increased.

It should be pointed out that there is uncertainty in the combustor equivalence ratio measurements during the DVT series.[2] There is evidence (from the comparison of calculated and measured generator performances, and from discrepancies between the calculated and measured concentrations of $O_2$ and $CO_2$ in the stack gas) to indicate that the actual values of combustor equivalence ratio are lower (i.e., more fuel rich) than the measured values shown in Figure 7. Whatever the magnitude of equivalence ratio, though, the generator channel fluctuations tended to decrease at higher values of equivalence ratios over the range o stoichiometry tested.

## III. HARDWARE CONDITION

The $1A_4$ generator channel, nozzle, and diffuser have accumulated more than 360 hours of operation as of this writing (May 1, 1993), includin 200 hours at the design power condition. The prototypic MHD hardware performed well throughout th DVT series. Some problems did arise early in the DV but they occurred either outside the generator chann (nozzle erosion and diffuser shorting) or were associated with the limitations of the nondestructiv inspection technique used for some of the fabricated parts (i.e., a few lifted caps on the electrodes). These problems were not life-threatening to the MHD generator and corrective measures have been implemented. These issues will be discussed later.

The overall physical condition of the generato channel is good. Many of the design features which were incorporated into the $1A_4$ have contributed to the overall soundness of the channel.

The channel wall box structure has proven to b airtight. Carbon monoxide (CO) sensors in the magne bore have consistently read zero throughout the DVT series. The absence of any trace of CO indicates th the gas seals on the channel walls are tight. A pressure leak rate check was performed on the channe box following the initial 50 hours of DVT. Results this test also indicated that all gas seals were intact. Fabricating each of the walls as a single unit minimized the number of required gas seals, compared to previous channel designs. This design feature also contributed to the pneumatic integrity the $1A_4$ channel.

The wall corner seals are all in good condition. No signs of degradation of the joint sea were evident during $1A_4$ channel disassembly. Corner joint problems were common in previous channel build ($1A_1$) at the CDIF because of arc damage and undercutting due to gas impingement. The problem of sidewall-to-electrode wall arcing was overcome by th use of aluminum nitride (AlN) ceramic tiles at the corner joints. This eliminated the necessity of having the rubber cement joint seal also act as an electrical insulator. The AlN ceramic elements were brazed onto the ends of the water-cooled electrodes and thus remained cool, further reducing the potenti for arcing at the corners. None of the corner ceramics were worn or cracked.

Significant effort was made during the design the $1A_4$ to streamline the exterior packaging of the channel. Layouts of the water cooling hoses, coolin manifolds, support brackets, wiring and wiring connection panels were carefully arranged in order t ease magnet closure. These efforts have resulted in reduced time for channel installation at the facility. Moreover, there have been no instances of pinched hoses or wires, or of magnet interference problems during the DVT.

The condition of the channel sidewalls is good Excellent slag coverage was obtained on both sidewalls. During the detailed channel inspection o November 1992, evidence of slight wear was noticed o the tops of some of the sidewall end bars. However, the amount of wear was not excessive given their 100 thermal hours of operation. There was also no

indication of undercutting of the sidebars or problems at the sidewall/cathode wall corner joints. Based on these observations, sidewall lifetime can be extrapolated well beyond the 2000-hour design requirement.

The cathode wall is also in very good condition. The cathode wall slag coverage has been excellent and there is no evidence of wear. The condition of this wall suggests that the 2000-hour lifetime requirement will be easily met.

The condition of the anode wall was satisfactory at the conclusion of Design Verification Testing given the sometimes adverse conditions it experienced. Large fluctuations in interanode voltages were experienced throughout much of the DVT, as mentioned earlier. This behavior suggests strong arcing at the anode wall surface. Also, very high interanode voltages (80 to 140 volts) were frequently measured during the test series. At such high gap voltages, arcing between the anodes is inevitable. Previous experience during subscale generator testing at Textron has shown that arcing appears when IAV's are in excess of 60 to 80 volts. In spite of these large interanode voltages, no permanent shorts have occurred on the $1A_4$ anode wall. This indicates that the fault protection features of the anode design (arc stretching grooves and a noncharring G-7 back wall) have worked successfully.[6] Marbling of the platinum top cap, like that seen during Textron Mk-VII and CDIF $1A_1$ materials confirmation tests, appeared on some anodes. However, this wear is a result of normal channel slagging operation and is not life-threatening. Some of the anode platinum top caps have lifted. The damage to these caps is related to manufacturing procedures and is not associated with the operation of the generator, as will be discussed later.

The current control devices operated well during the DVT series. The analysis and summary of their performance are reported in Reference 3. The circuits performed with no failures under nominal generator operating conditions, as well as during voltage and current transients resulting from emergency shutdowns of tests. The few circuit failures that occurred during the DVT series were directly attributable to transients from inverter trips and/or local open-circuits in wiring external to the current control circuits.

Overall, the $1A_4$ generator channel and associated hardware performed very well throughout the DVT series. As mentioned earlier, though, there were three problem areas identified during the DVT series. These are described below, as well as the corrective measures that were implemented to achieve subsequent successful testing.

Nozzle Wall Erosion

Early in the DVT series, localized damage was found in the lower right sidewall/bottom wall corner region of the inlet nozzle. The bulk of this damage occurred along the path of an axial streamer (about 18 inches long) extending from the nozzle throat to the inlet of the channel. See Figure 8. All of the damaged bars were water-cooled, copper based elements with a 0.375" thick tungsten cap. Throughout the early DVT series, it was also observed that this region of the right nozzle sidewall heat flux was higher than that of the left wall, sometimes by as much as 40 percent.

Two types of surface effects were noticed in the worn regions of the nozzle which suggest two different wear mechanisms. Most of the nozzle wear, particularly in the region of the elongated streamer shaped cavity, had a smooth polished appearance on the surface (Figure 9). This wear appeared to result from erosion by the plasma flow or by the iron oxide wake. Conversely, the wear region located closer to the lower corner of the nozzle had a very rough (orange peel-like) appearance. Metallurgical evaluation of the sidebars removed from this region suggested that the surface wear resulted from oxidation of the tungsten (forming tungstates, $WO_3$), followed by corrosion of the tungsten oxide. The oxidation of the tungsten caps might have occurred from a reaction with oxygen-rich wakes originating from the second-stage combustor duct. None of the wear was electrical in origin. The most significantly worn elements of the nozzle were replaced during the November 1992 generator channel inspection period.

Several of the tests during the DVT series were devoted to identifying the cause(s) of nozzle wall erosion. Specifically, this wear problem was addressed by varying the iron oxide injector locations and the number of second-stage oxygen injector nozzles, and their diameters, to improve flow mixing. These modifications reduced flow asymmetry, as indicated by the nozzle sidewall heat flux measurements. In addition, to prevent the iron oxide injectors from plugging due to improper installation, they were modified to insure that they can be set in position in a consistent manner from test to test. After the 93-DVT-28 test, the iron oxide injection ports were relocated further upstream in the second-stage combustor duct, away from the nozzle throat. The nozzle wear rate has slowed significantly (or stopped entirely) as a result of the recent hardware modifications.

Strong secondary flows (corner vortices and swirling flows leaving the combustor and intensified by the converging subsonic nozzle) have also been postulated as an additional possible cause of the observed nozzle wall erosion.[7] Efforts have been initiated to fabricate nozzle elements with a more gradual variation in the nozzle cross-sectional area. However, the fact that recent inspections of the nozzle have indicated that wear has slowed substantially (or even stopped) suggests that corner vortices may not be a major contributor to nozzle wear. This will be verified by more careful wear measurements during the next channel inspection and refurbishment period.

Electrical Shorting in the Diffuser

The power test 93-DVT-36 (March 1, 1993) was terminated as a result of a gas leak in the supersonic diffuser, just downstream of the channel/diffuser interface. From analysis of operational data and a post-test inspection of the diffuser, it was determined that the gas leak was due to failure of the G-11 back wall caused by electrical shorts and circulating currents in the diffuser.

A review of electrical data indicated that the shorts in the diffuser started during the first power generation test after the November 1992 channel/diffuser rebuild. Figure 10 shows the variation in the measured anode and cathode wall

voltage distributions at the aft end of the channel. At the start of the test, the Faraday voltages in the segmented diffuser section were in excess of 80-100 volts. Immediately after the start of the test, the measured Faraday voltages dropped steadily for 40 minutes, at which time the Faraday voltages were all less than 30 volts. This decrease in the Faraday voltages resulted from an electrical short located at the second diffuser frame downstream from the channel/diffuser interface. These reduced Faraday voltages persisted throughout all subsequent tests up to and including test 93-DVT-36. The results of Figure 10 suggest that the existing diffuser design and construction method did not provide the insulation necessary to sustain the Faraday voltage generated by the fringe magnetic field. The existing transverse segmentation (3 insulator gaps) is too coarse.

The external electrical loading was reconfigured to better distribute the Faraday voltage in the diffuser. This was done by adding Faraday load resistors between the diffuser sidebars, thus allowing some currents to circulate in exchange for high gap voltages. In addition, Faraday grading resistors were added to the last few channel electrodes to minimize the voltage mismatch present at the channel/diffuser interface. In order to repair the diffuser and resume the duration testing as quickly as possible, a noncharring G-7 fiberglass liner (similar to the liner used in the channel) was placed under the first four bar frames of the diffuser to prevent possible electrical shorting of the back walls.

This solution for controlling the diffuser voltage is working well. There have been no indications of electrical breakdowns or shortings during recent power tests.

Lifting of the Anode Platinum Top Caps

During the generator inspection at the completion of the initial DVT series in November 1992, it was discovered that the platinum top caps had separated from approximately 5 percent of the platinum-clad tungsten anode caplets. The lifting of the platinum top caps appeared to have been initiated by the failure of the braze joint and the resulting separation of the cap at the trailing edge of the caplets. An enlarged view of a partially lifted cap is shown in Figure 11. This separation of the top cap eventually leads to melting of the platinum from overheating. About 126 out of the total 2200 Pt/W caplets on the anode wall were found to be missing all or part of the platinum top cap as a result of this type of braze deficiency. None of the anodes with missing platinum top caps were replaced at the time of the channel inspection, although some of the partially lifted caps were removed. The $1A_4$ generator channel was then reboxed to allow the continuation of DVT.

Records of the anode fabrication and brazing histories were reviewed in an attempt to correlate lifted top caps to specific fabrication techniques and/or oven braze cycles. Nearly 70 percent of the lifted anode caps were produced in fewer than 10 percent of the Pt/W caplet subassembly braze cycles. The remainder of the platinum cap losses appear to be random, and most likely represent the "infant mortality" failures anticipated during the DVT series.

The loss of platinum anode top caps is not life-threatening to the ITC generator tests. At the time of the anode wall inspection, in November 1992, there was no evidence of any wear on the exposed tungsten surfaces where the platinum cap material was missing. The purpose of the back-up tungsten capping is precisely to protect the anodes against the possible loss of the platinum top caps. The results of materials duration tests carried out previously in the Textron Mk-VII MHD facility have indicated that the prototypic anode design can operate in excess of 1400 hours in the absence of a Pt top cap.[8]

## IV. DURATION TEST OPERATING CHARACTERISTICS

Duration test operating conditions and preliminary test results are presented. These results show typical operating characteristics of the $1A_4$ generator in POC duration tests conducted to date. At the nominal generator operating condition (shown in Table 2), the required prototypic values of channel wall stresses are achieved and fluctuations in the electrical parameters are minimized. It should be noted that the values of the equivalence ratios shown in Table 2 are based on measured process flows. As mentioned earlier, there is evidence to suggest that actual values of stoichiometry are somewhat lower.

Figures 12 and 13 show typical measured electrode current and interanode voltage distributions at the operating conditions of Table 2. The uniformity of the electrode current distribution indicates that the current controls are performing as intended. Interanode voltages are within allowable limits, and the absence of permanent electrical shorts suggests that the boron nitride insulators are in good condition. Also shown in these figures are the values of the prototypic current density ($J_y$) and axial electric field intensity ($E_x$).

Figure 14 shows a typical measured intercathode voltage profile. These voltages are all within acceptable bounds (less than 70 V). The near absence of slag shortings indicates that the iron oxide injection system is effective in preventing slag polarization.[9]

The measured electrical characteristics of the generator during duration testing are relatively smooth, as illustrated in Figures 15 and 16. Figure 15 shows the level of mid-channel interanode voltage fluctuations, $\chi$ , and Figure 16 shows the amount of load current fluctuations, $\tau$ . Both figures are based on a one-hour period from test 93-POC-8. This test had over 20 hours of uninterrupted power operation with steady electrical characteristics throughout. The degree of IAV fluctuations is substantially lower than those observed in earlier Design Verification Tests, as seen by comparing Figure 15 to Figure 6(a). The level of fluctuations in the load current was also reduced substantially in recent POC tests, as seen by a comparison of Figures 16 and 7(a).

Inspections of the generator channel gas-side surfaces have shown no evidence of unusual wear or signs of water leaks. In addition, there have been no indications of any reduction in the channel electrical integrity.

Inspection of the nozzle area is performed at every opportunity. No discernible increase in wear has been observed since the oxygen port reconfiguration was completed. In addition, the performance of the forward segmented diffuser has continued to be good throughout duration testing. The placement of resistors between the sidebars is

effective in redistributing the Faraday voltage between the transverse diffuser segments. Also, the Faraday voltage in the diffuser region remains steady, indicating an absence of internal shortings.

## V. SUMMARY

The purpose of the Design Verification Test was to assure the readiness of the prototypic hardware for POC duration testing and to verify operating conditions to be used during the duration test. Early Design Verification Testing consisted of facility shakedown and combustor optimization, which frequently resulted in off-design operation and harsh operating conditions for the generator channel. The problems were resolved in later Design Verification Tests. Power train operation grew smoother, tests of longer duration were possible, and performance (as characterized by power, conductivity and the degree of fluctuation of electrical properties) improved dramatically. At the completion of DVT, "infant mortality" problems had been identified and eliminated, and nominal operating conditions for the duration test had been verified.

Proof-of-concept testing is now well underway. To date, over 360 hours of the planned 1000 hours of testing has been completed. Generator testing is being performed at operating conditions representative of commercial plant operation. Power train operation is very smooth and prototypic channel hardware, shown in Figures 17 and 18, is performing very well.

Based on test results obtained thus far, the prognosis is excellent for meeting all of the POC test objectives.

## VI. REFERENCES


1. TRW, "Test Plan for Design Verification and Duration Testing of the Prototypical Coal-Fired MHD Powertrain," TRW Document No. MHD-ITC-92-134, June 8, 1992.

2. Myrick, S., et al., "50 $MW_T$ Prototypical Combustor Performance," 31st Symp. Engineering Aspects of MHD, Whitefish, MT, June 1993.

3. Reich, J.E., et al., "Summary and Analysis of Prototypic Current Control Performance at the CDIF," 31st Symp. Engineering Aspects of MHD, Whitefish, MT, June 1993.

4. Myrick, S., et al., "Coal-Fired MHD Power Train Performance Test Results," Proc. 26th Symp. Engineering Aspects of MHD, Nashville, TN, June 1988.

5. Daniel, V.W., et al., "Spectral Analysis of CDIF Test Data," 31st Symp. Engineering Aspects of MHD, Whitefish, MT, June 1993.

6. Pian, C.C.P., et al., "Design and Fabrication of the Prototypic MHD Generator for the Integrated Topping Cycle," 11th Int. Conf. on MHD Electrical Power Generation, Beijing, PRC, October 1992.

7. Solbes, A., "Secondary Flows and Nozzle Contours for the $1A_4$ Power Train," TRW Interoffice Correspondence No. K318.93.AS.004, Feb. 1, 1993.

8. Pollina, R.J., et al., "$1A_4$ Materials Corrosion and Confirmation Test Results," 29th Symp. on the Engineering Aspects of MHD, New Orleans, LA, June 1991.

9. Petty, S.W., et al., "Coal-Fired MHD Channel Parametric Studies, Aspects of Power Generation with Iron Oxide Addition," 27th Symp. on the Engineering Aspects of MHD, Reno, NV, June 1989.


**Table 1**

Summary of Operating Conditions and Model Assumptions

| | Pre-Test Calculations (Stress ROC) | 92-DVT-10 bt = 15:47-16:00 |
|---|---|---|
| Oxidant N/O | 0.84 | 0.82 |
| 1st-Stage Equivalence Ratio | NA | 0.55 |
| 2nd-Stage Equivalence Ratio | 0.90 | 0.91 |
| Seed Fraction (wt. % K) | 1.7 | 1.83 |
| Iron Oxide Slurry (lb/min) | --- | 4.0 |
| Combustor + Nozzle Heat Loss (% thermal input) | 8.75 | 8.0 |
| Gas Conductivity at Nozzle Throat (mho/m) | 7.5 | ? |
| Power (MWe) | 0.97 | 1.02 |
| Load Current (A) | 178. | 182. |
| Load Voltage (kV) | 5.4 | 5.6 |
| Assumed Constant Wall Leakage Current (A) | 90. | NA |
| Assumed Wall Resistance (ohms/gap) | 1.2 | NA |

P7075

**Table 2**

Nominal POC Duration Test
"Stress" Operating Conditions

Combustor Parameters

| | |
|---|---|
| Vitiator Preheat | 2900 °F |
| CFPC Stoichiometry | 0.64 |
| Stage 1 Stoichiometry | 0.55 to 0.58 |
| Stage 2 Stoichiometry | 0.95 to 0.98 |
| Seed Oxygen Carrier | 1900 lbm/hr |
| Seed | 1.8 wt. % K |
| Burner Pressure | 6.0 Atm |

MHD Generator Parameters

| | |
|---|---|
| Power Output | 1.0 MW |
| Load Current | 200 A |
| Load Voltage | 5.0 - 5.5 kV |
| Maximum $J_y$ | 0.7 A/cm$^2$ |
| Maximum $E_x$ | 2.1 kV/m |
| Maximum Heat Flux | 250 W/cm$^2$ |
| Iron Oxide Slurry | 5.0 lbs/min |

P7076

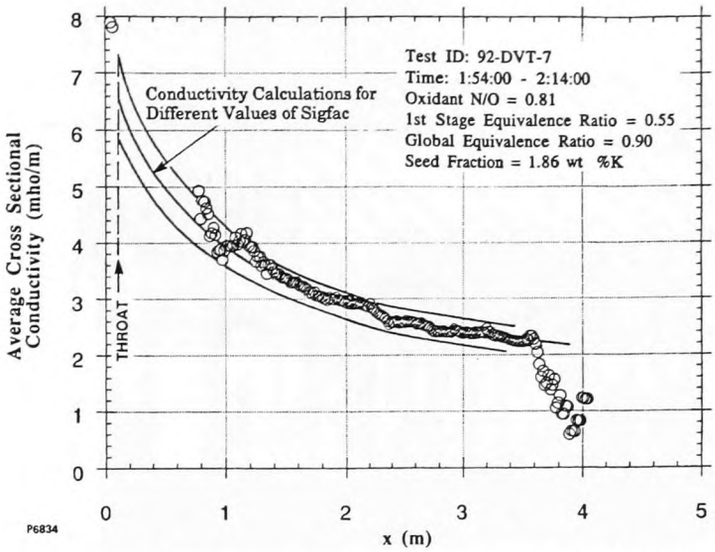


Figure 1 Typical Measured Conductivity Profile for CDIF $1A_4$ Generator Channel.

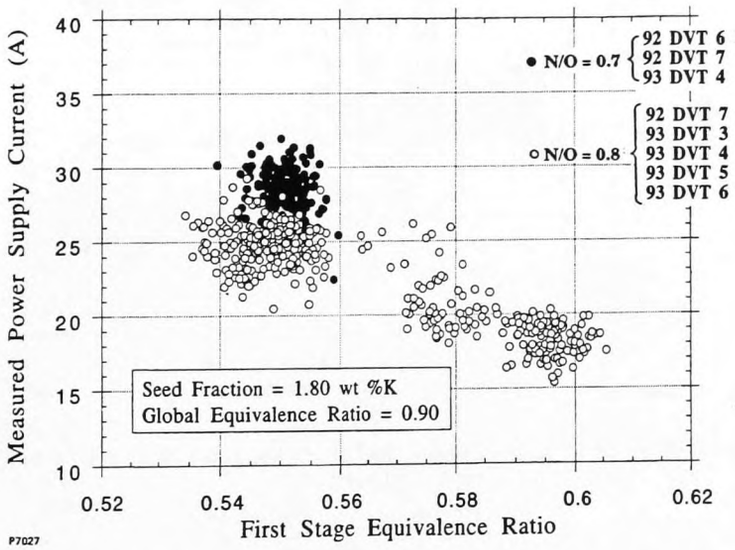


Figure 2 Measured Power Supply Current as a Function of First Stage Equivalence Ratio. Early DVT Series.

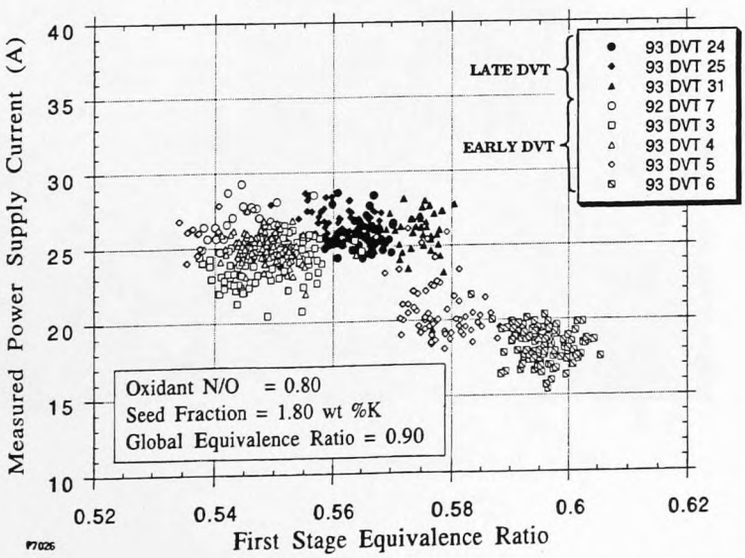


Figure 3 Measured Power Supply Current as a Function of First Stage Equivalence Ratio for N/O = 0.8. Early and Late DVT Series.

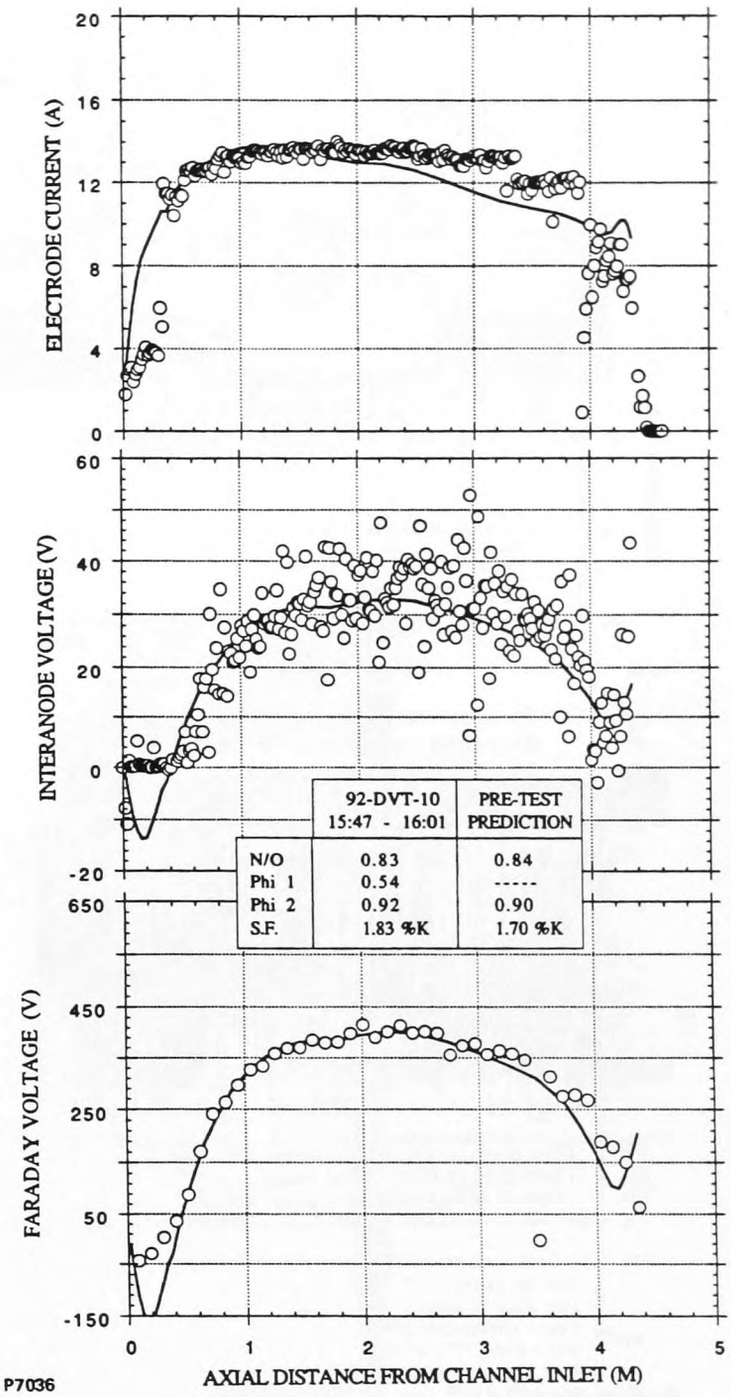


Figure 4 Comparisons of Measured and Calculated Electrode Current, Interanode Voltage, and Faraday Voltage Distributions.

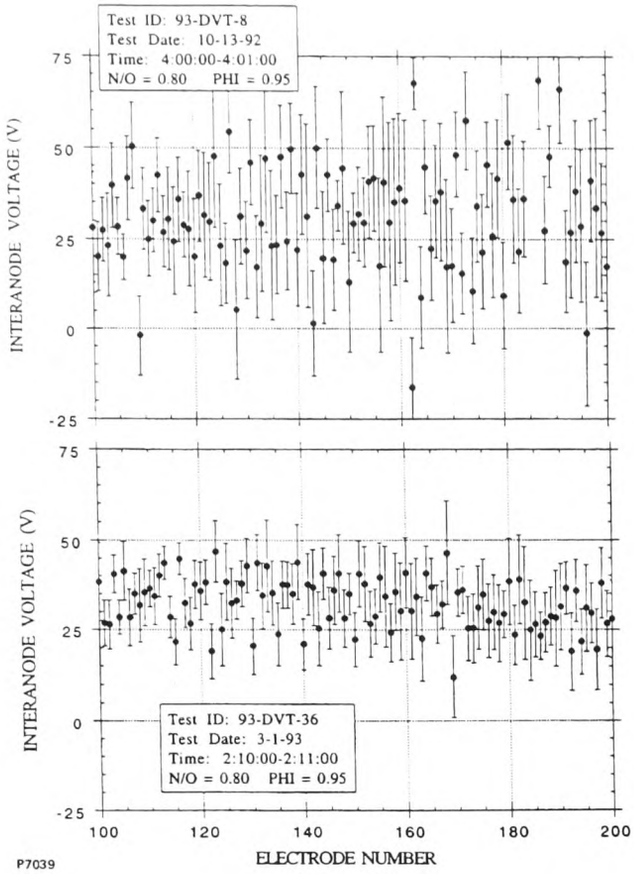


Figure 5 Streamwise Distributions of Mean and Standard Deviation of IAV from Tests 93-DVT-8 and 93-DVT-36.

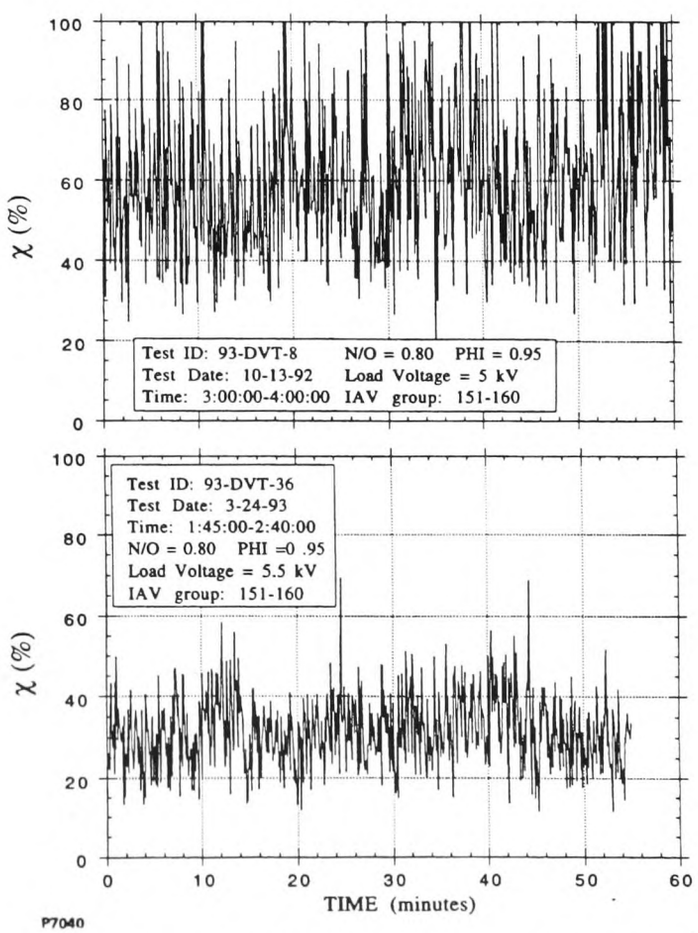


Figure 6 Interanode Voltage Fluctuations Versus Time from Tests 93-DVT-8 and 93-DVT-36.

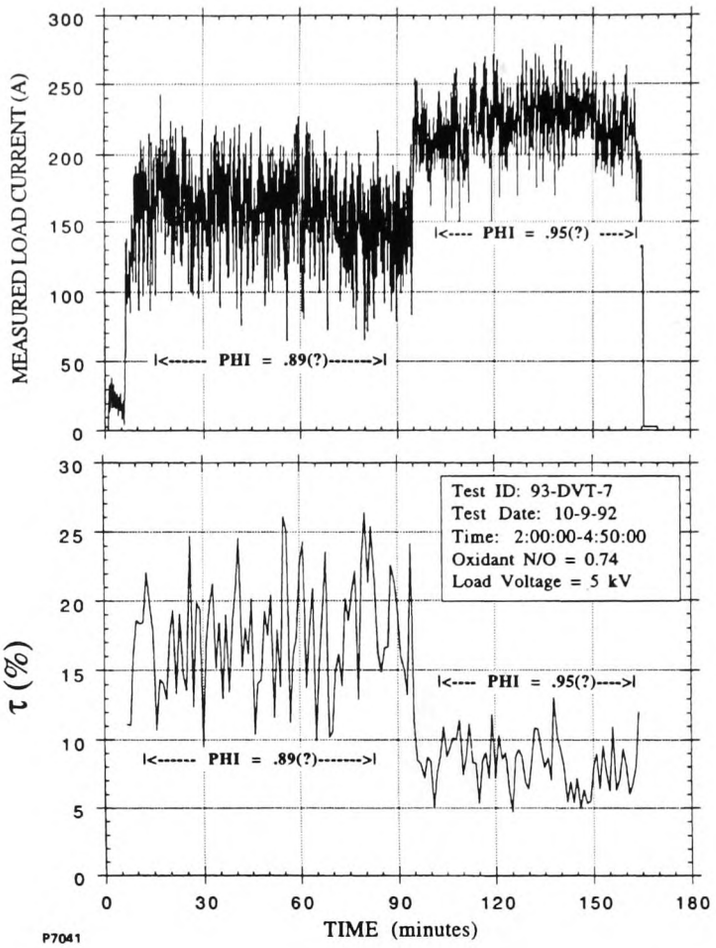


Figure 7 Equivalence Ratio Effect on Measured Load Current Fluctuations.

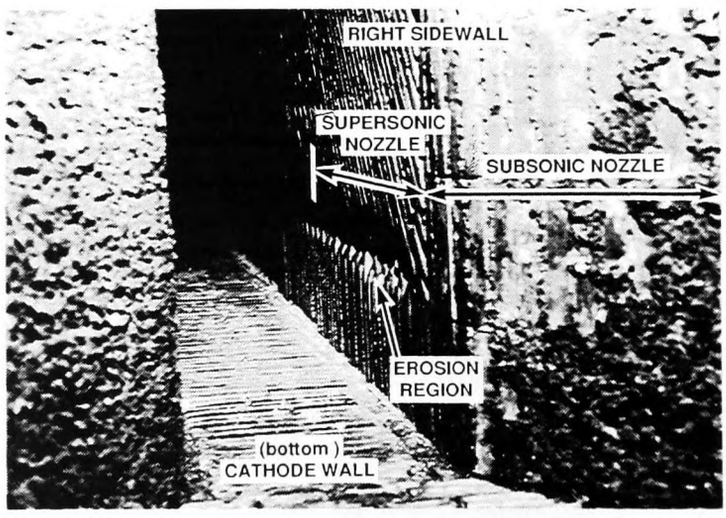


Figure 8 Photograph of Nozzle Erosion.

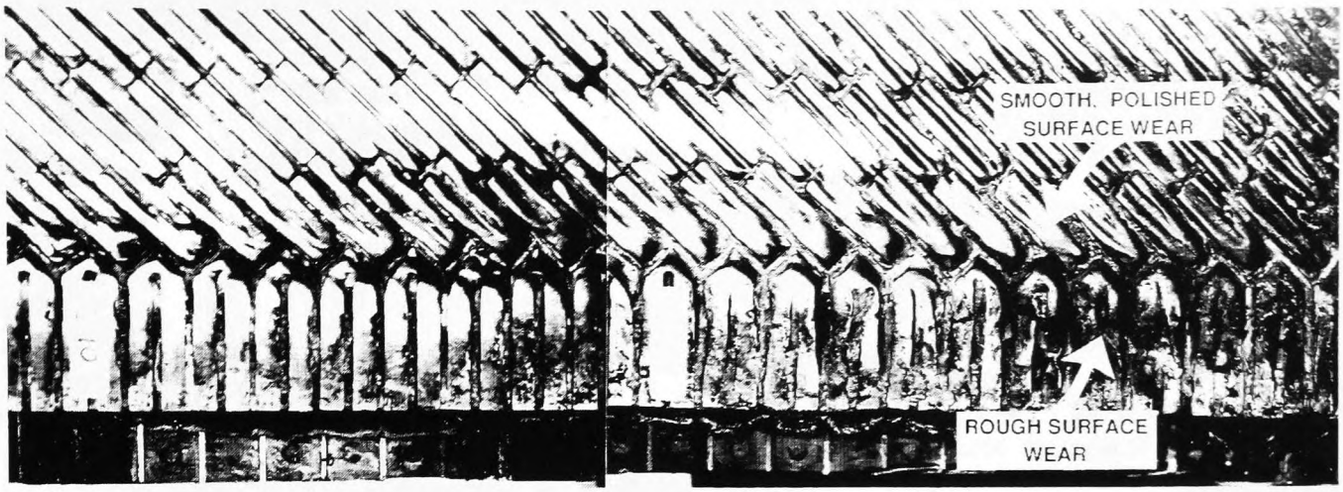


Figure 9 Details of the Right Sidewall Nozzle Wear.

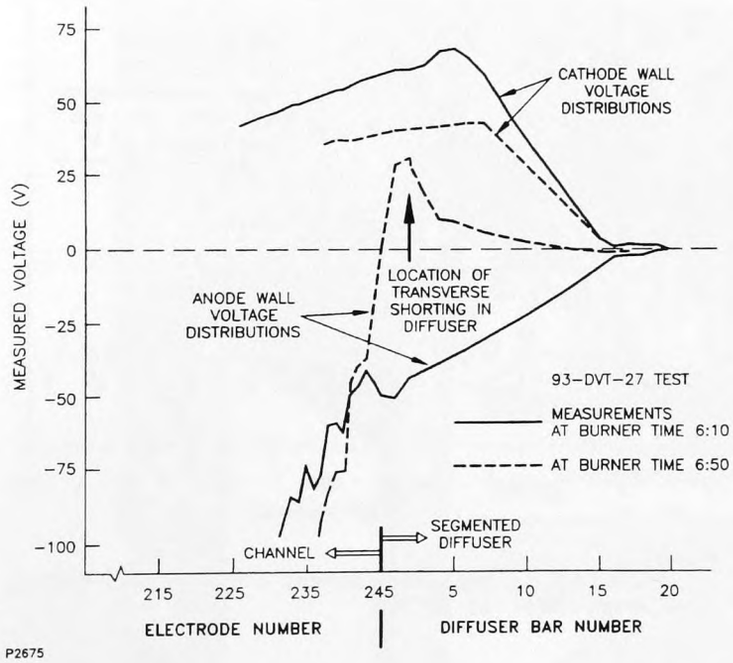


Figure 10 The Measured Voltage Distributions in the Diffuser During 93-DVT-27 Test.

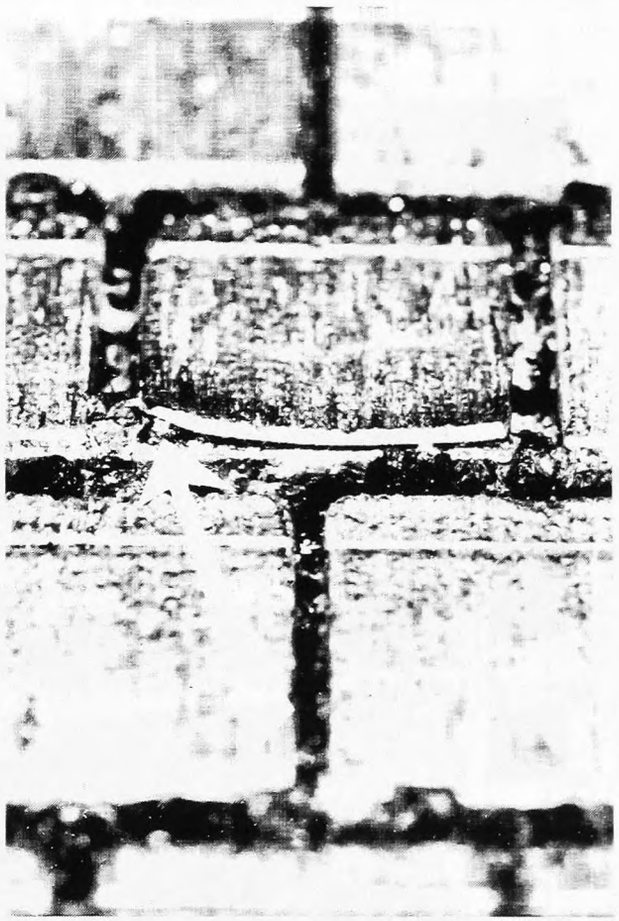


Figure 11 A Close-Up View of the Lifted Trailing Edge of a Platinum Top Cap.

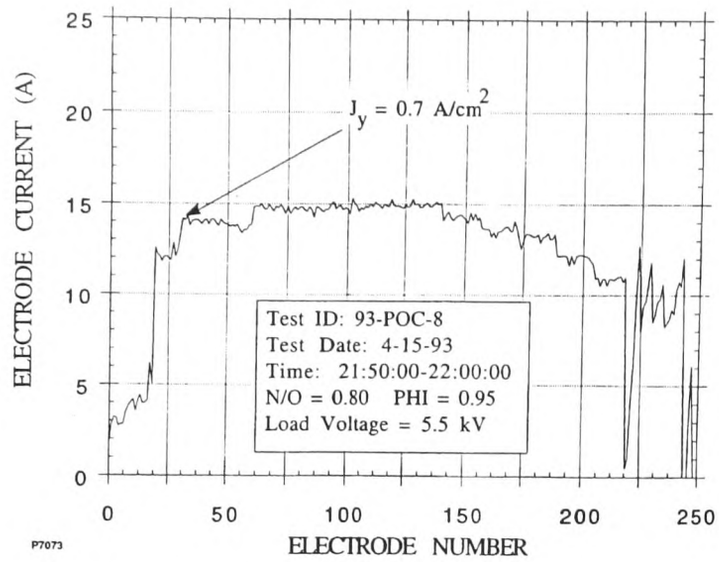


Figure 12 Typical Electrode Current Distribution for a POC Duration Test.

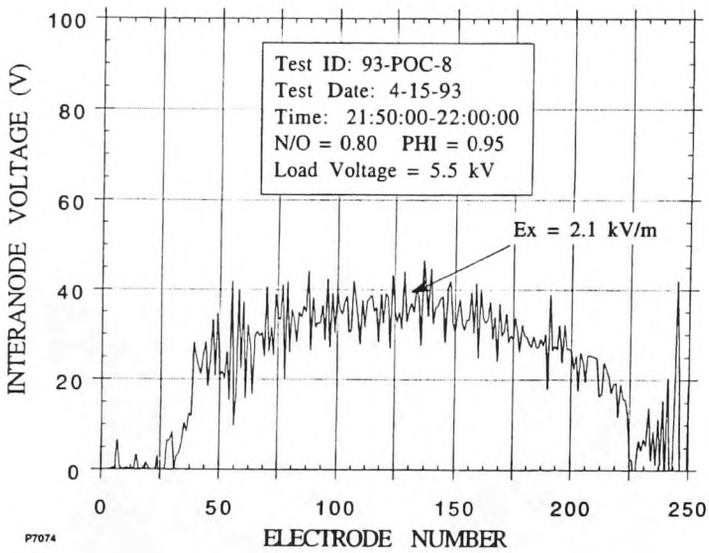


Figure 13 Typical Interanode Voltage Distribution for a POC Duration Test.

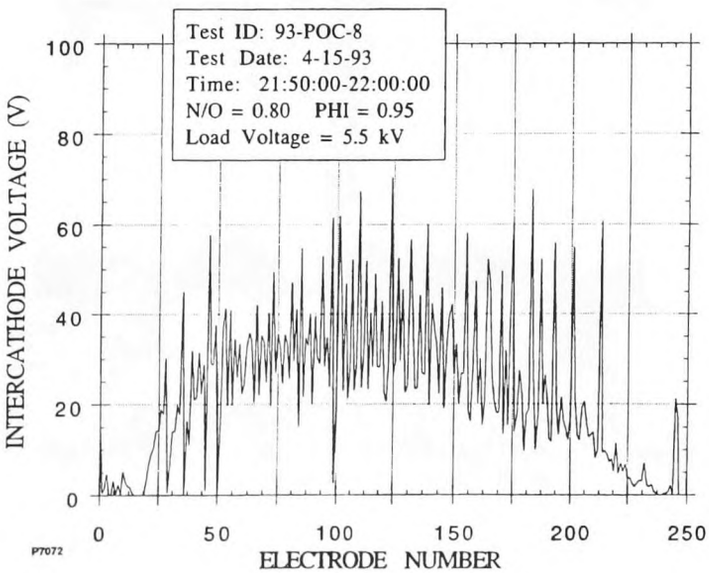


Figure 14 Typical Intercathode Voltage Distribution for a POC Duration Test.

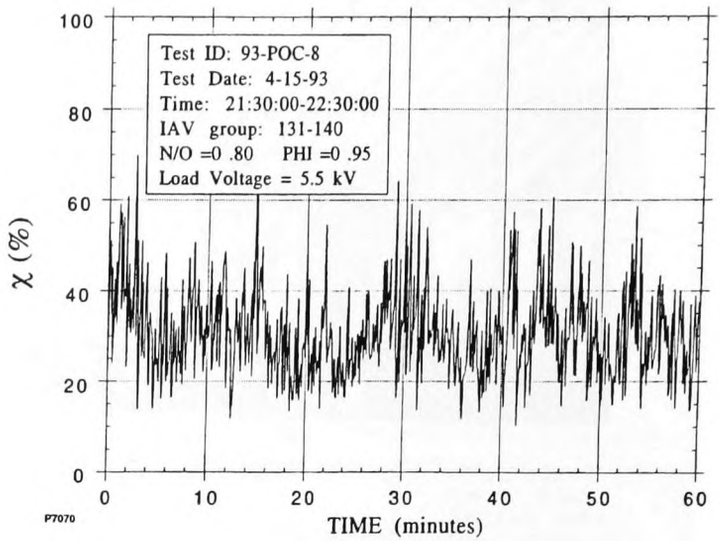


Figure 15 Interanode Voltage Fluctuations Versus Time from Test 93-POC-8.

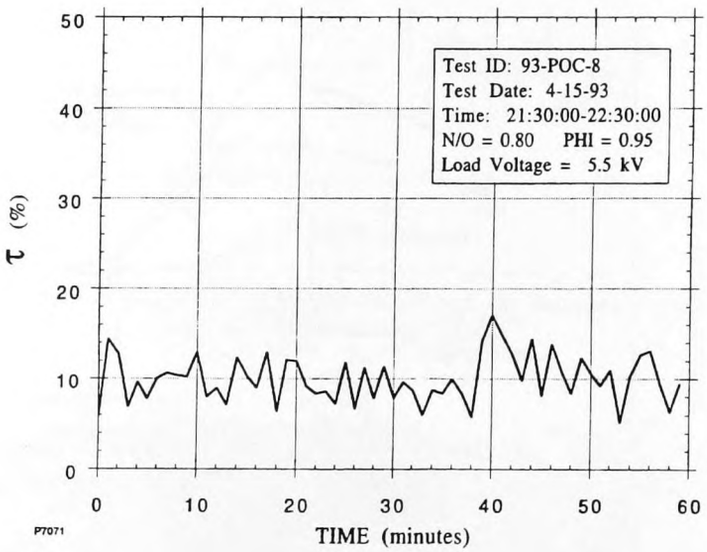


Figure 16 Measured Load Current Fluctuations During Test 93-POC-8.

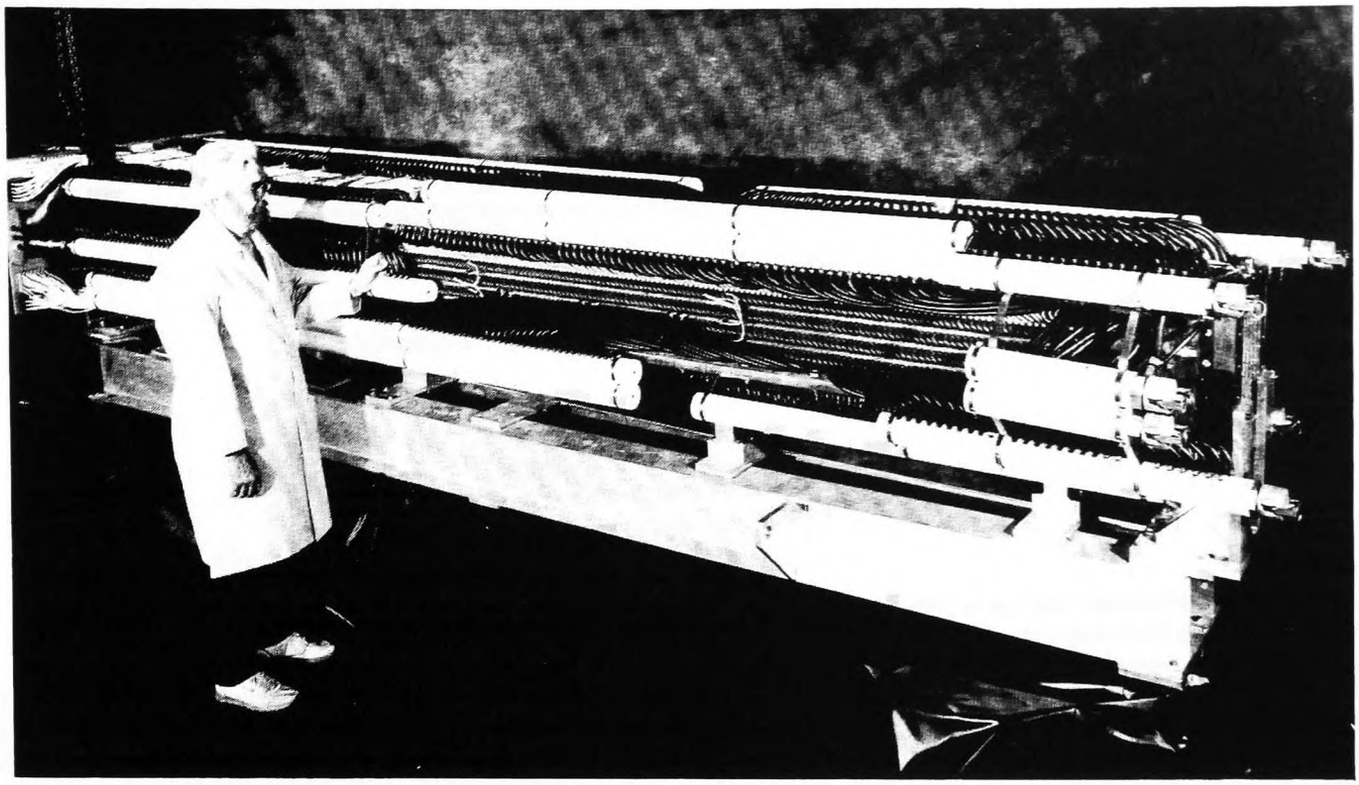

Figure 17 $1A_4$ Prototypic MHD Generator Channel

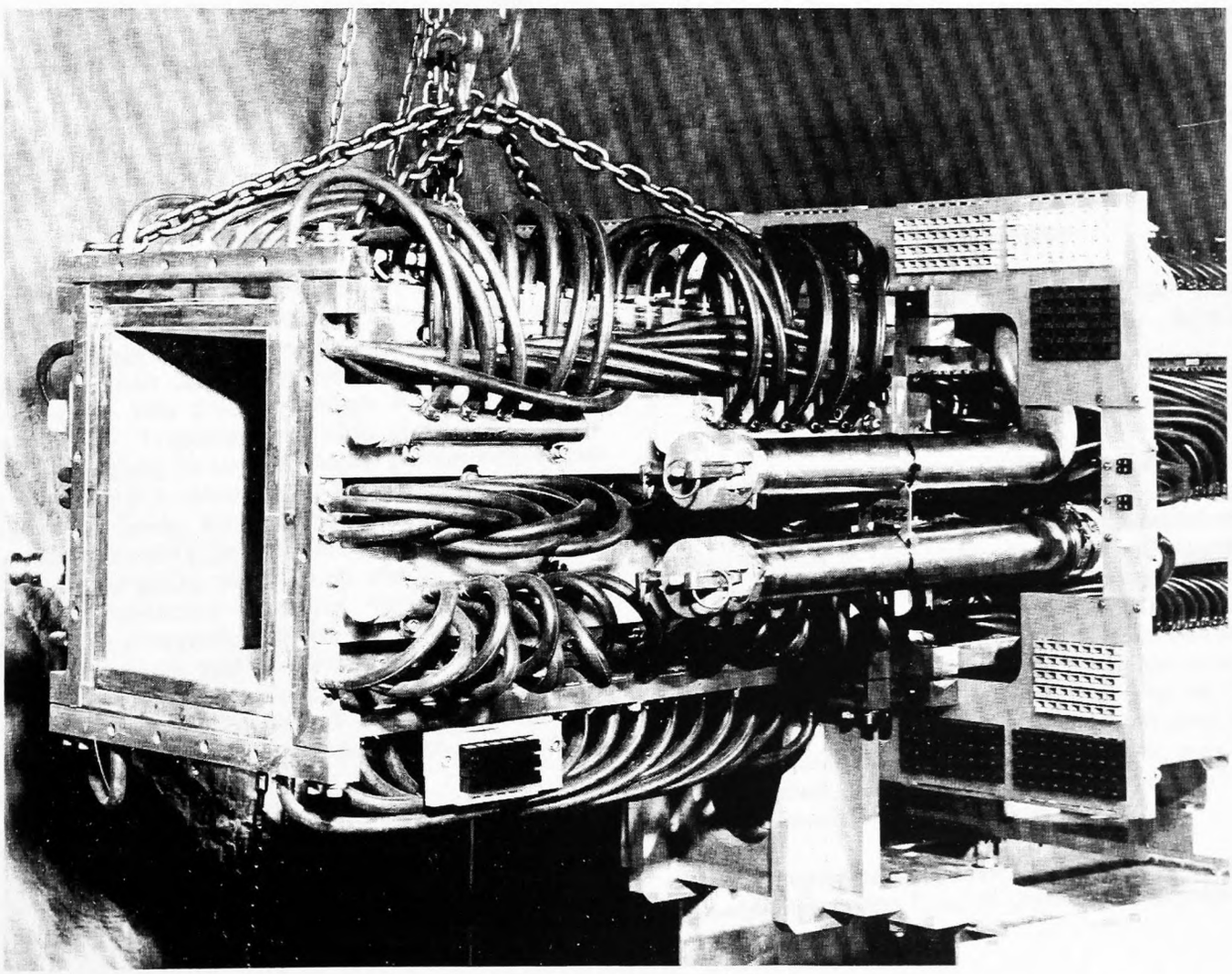

Figure 18 $1A_4$ Segmented Supersonic Diffuser